



Short communication

LiMn_{0.8}Fe_{0.19}Mg_{0.01}PO₄/C as a high performance cathode material for lithium ion batteries

Haisheng Fang^{a,b,c,*}, Enrui Dai^{a,b,c}, Bin Yang^{a,b,c}, Yaochun Yao^{a,b,c}, Wenhui Ma^{a,b,c}^a Faculty of Metallurgical and Energy Engineering, Kunming University of Science and Technology, Kunming 650093, China^b National Engineering Laboratory for Vacuum Metallurgy, Kunming University of Science and Technology, Kunming 650093, China^c Key Laboratory of Nonferrous Metals Vacuum Metallurgy of Yunnan Province, Kunming University of Science and Technology, Kunming 650093, China

ARTICLE INFO

Article history:

Received 15 November 2011

Received in revised form

12 December 2011

Accepted 20 December 2011

Available online 30 December 2011

Keywords:

Lithium ion batteries

Cathode

Lithium manganese phosphate

Cation substitution

ABSTRACT

A new LiMnPO₄ based material, LiMn_{0.8}Fe_{0.19}Mg_{0.01}PO₄/C, is synthesized by a solid state method and characterized by X-ray diffraction (XRD), scanning electron microscopy (SEM) and electrochemical test. The obtained LiMn_{0.8}Fe_{0.19}Mg_{0.01}PO₄ crystals with 8 wt.% carbon coating are mainly 100–500 nm in size, and aggregate into microparticles around 3–5 μm. The electrochemical test demonstrates that the obtained LiMn_{0.8}Fe_{0.19}Mg_{0.01}PO₄/C has high capacity, good cycleability and quite excellent rate capability in spite of its larger size and less carbon coating as compared to those reported in the previous works. When discharged at a high rate of 10C, the obtained LiMn_{0.8}Fe_{0.19}Mg_{0.01}PO₄/C can still deliver a capacity of 115 mAh g⁻¹. The results prove that the LiMn_{0.8}Fe_{0.19}Mg_{0.01}PO₄/C is a very promising cathode material for lithium ion batteries.

© 2011 Elsevier B.V. All rights reserved.

1. Introduction

Recently, there is an increasing interest in LiMnPO₄ because it offers promise to replace the expensive LiCoO₂. However, the electrochemical performance of LiMnPO₄ especially the rate performance was seriously limited by its extremely slow electron and ion conduction [1–4]. Several classic methods including carbon coating [5–8], particle size reduction [9–11] and cation substitution [12–18] have been adopted to improve the performance of LiMnPO₄, but only few groups could attain high rate LiMnPO₄ based materials. To our knowledge, only two LiMnPO₄ based materials reported in the available literatures could discharge a capacity no less than 90 mAh g⁻¹ at the rate of 10C as yet [19,20]. In 2009, Martha et al. reported that the 20–100 nm LiMn_{0.8}Fe_{0.2}PO₄ crystals with 10 wt.% carbon coating had an excellent rate capability and could deliver a capacity of around 93 mAh g⁻¹ at the rate of 10C [19]. More recently, a much better rate capability was achieved on the wet chemistry derived LiMn_{0.75}Fe_{0.25}PO₄ nanorods (length 50–100 nm, width 20–30 nm) grown on the reduced graphene oxide sheets reported by Wang et al. [20]. It is noted that these two high rate LiMnPO₄ based materials are both based on the use of nanomaterials. However, recent findings revealed that the delithiated phase of LiMnPO₄ is thermally

unstable and reactive toward the electrolyte [21–26], and the use of nanoparticles would encounter more related problems due to the increased high surface area and high reactivity of smaller particles [22]. Moreover, the use of a large amount (20 wt.%) of the reduced graphene oxide as carbon source in Ref. [20] is undesirable for the consideration of cost and energy density. Therefore, developing high performance LiMnPO₄ based materials with larger size and less carbon coating is crucial for practical application.

More recently, we demonstrated that the rate performance of LiMnPO₄ could be significantly enhanced via Mn-site co-substitution with 10 at.% Fe and Mg, but the capacity fade at high rates (>2C) was still relatively rapid [27,28]. Although reducing particle size and/or increasing carbon coating content are technically feasible to further enhance the rate capability of LiMn_{0.9}Fe_{0.09}Mg_{0.01}PO₄, these methods will bring about some undesirable effects for practical application as mentioned before. Previous works reported that rate capability of the solid solution LiFe_xMn_{1-x}PO₄ increases with Fe content, but the energy density is peaked around $x=0.2$, and further increasing Fe content may reduce the energy density because of the lower redox potential of Fe²⁺/Fe³⁺ (3.4 V vs. Li/Li⁺) [19,29]. Based on these results, increasing Mn-site substitution by Fe and Mg to 20 at.% is tried out in the present work with an aim to enhance the rate capability of LiMnPO₄ without sacrificing energy density and safety. The results showed that the obtained submicron LiMn_{0.8}Fe_{0.19}Mg_{0.01}PO₄ crystals with carbon coating less than 10 wt.% could yield a high capacity mostly

* Corresponding author. Tel.: +86 871 5107208; fax: +86 871 5107208.

E-mail address: hsfang1981@yahoo.com.cn (H. Fang).

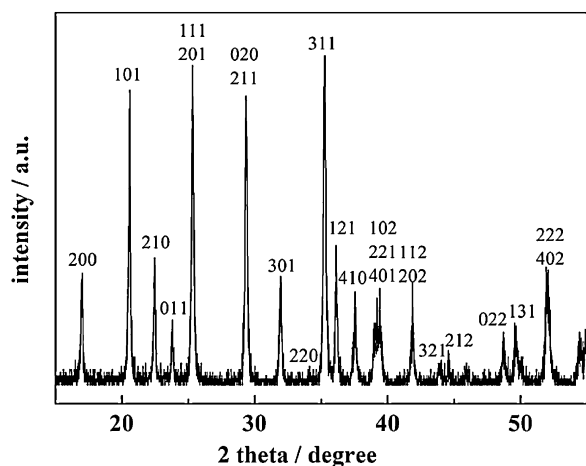


Fig. 1. XRD pattern of $\text{LiMn}_{0.8}\text{Fe}_{0.19}\text{Mg}_{0.01}\text{PO}_4/\text{C}$.

available in the high-voltage domain and a remarkably excellent rate capability with a discharge capacity of 115 mAh g^{-1} at the rate of 10 C.

2. Experimental

$\text{LiMn}_{0.8}\text{Fe}_{0.19}\text{Mg}_{0.01}\text{PO}_4$ was synthesized by a solid-state reaction. Chemicals of LiH_2PO_4 , $\text{MnC}_4\text{H}_6\text{O}_4 \cdot 4\text{H}_2\text{O}$, $\text{MgC}_4\text{H}_6\text{O}_4 \cdot 4\text{H}_2\text{O}$, $\text{H}_2\text{C}_2\text{O}_4 \cdot 2\text{H}_2\text{O}$ and $\text{FeC}_2\text{O}_4 \cdot 2\text{H}_2\text{O}$ were mixed with sucrose (14 wt.%) by ball-milling for 6 h. The milled mixture was dried and then heated at 800°C for 10 h under an Ar atmosphere. The carbon content of the product was around 8 wt.%.

The crystalline phase was identified by powder X-ray diffraction (XRD). The lattice parameters were calculated by refining the XRD patterns using Rietica. The morphology and particle size was observed by scanning electron microscopy (SEM). The carbon content was measured by the VarioEL III (elementar, Germany). Electrochemical measurement was conducted by assembly of 2025 coin-type cell with a lithium metal anode. The cathode was made by mixing active material, Super P and polyvinylidene fluoride (PVDF) in a weight ratio of 8:1:1. The electrolyte was 1 M LiPF_6 in EC/DMC (1/1) solution. All cells were assembled in an Ar-filled glove box. Cells were charged at a constant current–constant voltage (CC–CV) mode and then discharged at a constant current at 25°C .

3. Results and discussion

Fig. 1 shows XRD pattern of the prepared $\text{LiMn}_{0.8}\text{Fe}_{0.19}\text{Mg}_{0.01}\text{PO}_4/\text{C}$. All diffraction peaks can be fully indexed into an orthorhombic structure with a space group of $Pnma$. The absence of carbon peaks in the XRD pattern indicates the amorphous nature of the residual carbon pyrolyzed from the sucrose. The Fe and Mg co-substitution results in a crystal lattice shrink because of the smaller ionic radii of Mg^{2+} (0.66 Å) and Fe^{2+} (0.74 Å) as compared to that of Mn^{2+} (0.80 Å). The lattice parameters of the $\text{LiMn}_{0.8}\text{Fe}_{0.19}\text{Mg}_{0.01}\text{PO}_4$ were calculated by refining the XRD pattern with $a = 10.4263 \pm 0.0010 \text{ \AA}$, $b = 6.0824 \pm 0.0006 \text{ \AA}$, $c = 4.7334 \pm 0.0005 \text{ \AA}$. A comparison of lattice parameters of $\text{LiMn}_x\text{Fe}_{0.99-x}\text{Mg}_{0.01}\text{PO}_4$ is shown in Fig. S1 in Supplementary data. It is seen that the change of lattice parameters follows Vegard's law, which indicates that part of Mn atoms in LiMnPO_4 was successfully co-substituted by Fe and Mg leading to the formation of $\text{LiMn}_{0.8}\text{Fe}_{0.19}\text{Mg}_{0.01}\text{PO}_4$ solid solution. Fig. 2 shows SEM image of the prepared $\text{LiMn}_{0.8}\text{Fe}_{0.19}\text{Mg}_{0.01}\text{PO}_4/\text{C}$. It is seen that the primary crystals are mainly between 100 and 500 nm in size, and aggregate into microsize particles around 3–5 μm .

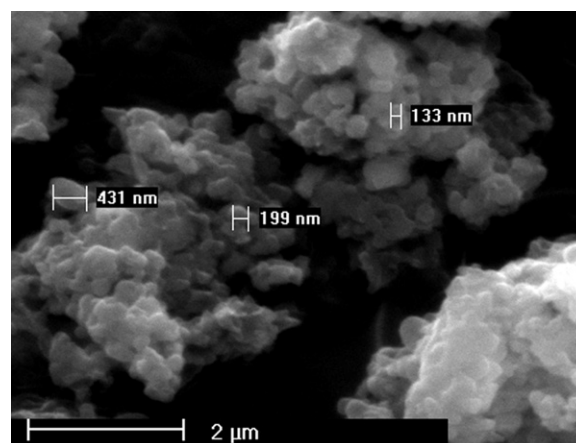


Fig. 2. SEM image of $\text{LiMn}_{0.8}\text{Fe}_{0.19}\text{Mg}_{0.01}\text{PO}_4/\text{C}$.

Electrochemical performance of the prepared $\text{LiMn}_{0.8}\text{Fe}_{0.19}\text{Mg}_{0.01}\text{PO}_4/\text{C}$ was evaluated using CR2025 coin-type cell and exhibited in Fig. 3. For comparison, related data of $\text{LiMn}_{0.9}\text{Fe}_{0.09}\text{Mg}_{0.01}\text{PO}_4/\text{C}$ are also presented. Fig. 3a and b display typical charge/discharge curves cycled at 0.2 and 1 C (equal to 150 mA g^{-1}), respectively. Corresponding cycling performance is shown in Fig. 3c. Cells were charged at 0.2 or 1 C to 4.5 V, held at 4.5 V until the current decreased to 0.02 C, and then discharged at 0.2 or 1 C to 2.5 V. As shown in Fig. 3a and b, two voltage plateaus around 4.1 and 3.5 V are clearly observed for $\text{LiMn}_{0.8}\text{Fe}_{0.19}\text{Mg}_{0.01}\text{PO}_4/\text{C}$. The flat and longer 4.1 V plateaus are related to the $\text{Mn}^{2+}/\text{Mn}^{3+}$ redox couple, and the smaller but obvious 3.5 V plateaus are related to the $\text{Fe}^{2+}/\text{Fe}^{3+}$ redox couple. However, the plateaus of the $\text{Fe}^{2+}/\text{Fe}^{3+}$ redox couple were almost invisible for $\text{LiMn}_{0.9}\text{Fe}_{0.09}\text{Mg}_{0.01}\text{PO}_4/\text{C}$ due to the small ratio of Fe [28]. Therefore, the observed 3.5 V plateaus indicate the increased ratio of Fe in LiMnPO_4 demonstrating the successful substitution of Mn by Fe in our prepared sample. When cycled at 0.2 C, the prepared $\text{LiMn}_{0.8}\text{Fe}_{0.19}\text{Mg}_{0.01}\text{PO}_4/\text{C}$ had a small polarization between the charge and discharge plateaus as shown in Fig. 3a, and could deliver a stable capacity around 140 mAh g^{-1} ($\text{LiMn}_{0.8}\text{Fe}_{0.19}\text{Mg}_{0.01}\text{PO}_4$ has a theoretical specific capacity of 169 mAh g^{-1} with a corresponding theoretical specific energy of 663 Wh kg^{-1}) as shown in Fig. 3c. When the rate increased to a commercially important rate of 1 C after 50 cycles at 0.2 C, the polarization potential was slightly increased (Fig. 3b), and the reversible capacity could still retain 132 mAh g^{-1} and faded very slowly in the subsequent 30 cycles (Fig. 3c). Moreover, it is clear that the $\text{LiMn}_{0.8}\text{Fe}_{0.19}\text{Mg}_{0.01}\text{PO}_4/\text{C}$ had much smaller polarizations between charge and discharge plateaus and much higher reversible capacities at both rates as compared to the $\text{LiMn}_{0.9}\text{Fe}_{0.09}\text{Mg}_{0.01}\text{PO}_4/\text{C}$, indicating the enhanced reaction kinetics.

Fig. 3d exhibits the rate capability of the prepared $\text{LiMn}_{0.8}\text{Fe}_{0.19}\text{Mg}_{0.01}\text{PO}_4/\text{C}$. Cells were charged at 0.1 C to 4.5 V, held at 4.5 V until the current decreased to 0.01 C, and then discharged at various rates to 2 V. It is seen that the $\text{LiMn}_{0.8}\text{Fe}_{0.19}\text{Mg}_{0.01}\text{PO}_4/\text{C}$ had a remarkably excellent rate capability which is much better than that of the $\text{LiMn}_{0.9}\text{Fe}_{0.09}\text{Mg}_{0.01}\text{PO}_4/\text{C}$. The reversible capacity of the $\text{LiMn}_{0.8}\text{Fe}_{0.19}\text{Mg}_{0.01}\text{PO}_4/\text{C}$ could reach 145 mAh g^{-1} at 0.1 C, 141 mAh g^{-1} at 1 C, 135 mAh g^{-1} at 3 C, 128 mAh g^{-1} at 5 C and 115 mAh g^{-1} at 10 C (95 mAh g^{-1} at a cut-off voltage of 2.7 V). Clearly, the rate capability of Fe and Mg co-substituted LiMnPO_4 could be significantly enhanced by a slight increase of Fe amount for Mn-site substitution, which is well consistent to the previous reports [29]. It is noted that the high rate capability of our $\text{LiMn}_{0.8}\text{Fe}_{0.19}\text{Mg}_{0.01}\text{PO}_4/\text{C}$ was achieved on the submicron crystals with carbon coating only about 8 wt.%. In most reported

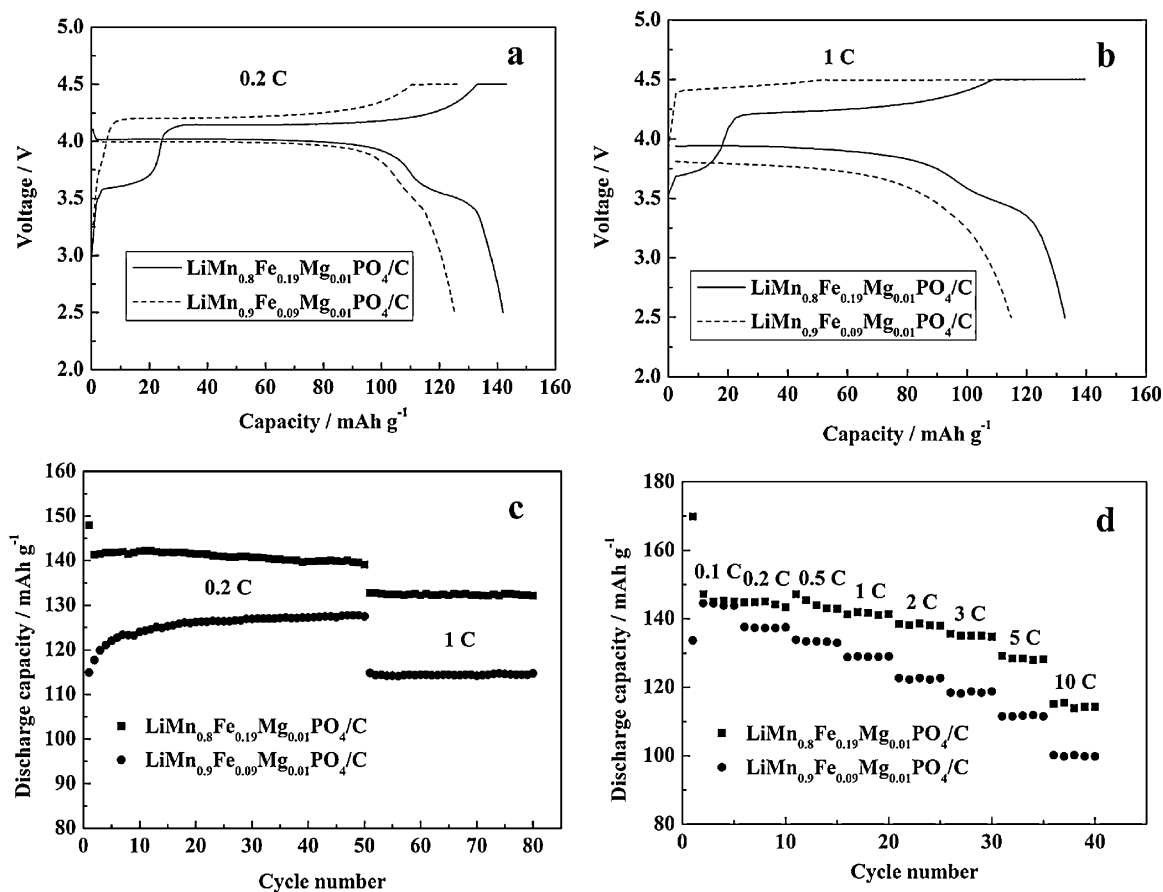


Fig. 3. Typical charge/discharge curves of $\text{LiMn}_{0.9}\text{Fe}_{0.09}\text{Mg}_{0.01}\text{PO}_4/\text{C}$ and $\text{LiMn}_{0.8}\text{Fe}_{0.19}\text{Mg}_{0.01}\text{PO}_4/\text{C}$ cycled at (a) 0.2 and (b) 1 C (equal to 150 mA g⁻¹), (c) cycling performance of $\text{LiMn}_{0.9}\text{Fe}_{0.09}\text{Mg}_{0.01}\text{PO}_4/\text{C}$ and $\text{LiMn}_{0.8}\text{Fe}_{0.19}\text{Mg}_{0.01}\text{PO}_4/\text{C}$ cycled at 0.2 and 1 C. Cells were charged at 0.2 or 1 C to 4.5 V, held at 4.5 V until the current decreased to 0.02 C, and then discharged at 0.2 or 1 C to 2.5 V. (d) Rate capability of $\text{LiMn}_{0.9}\text{Fe}_{0.09}\text{Mg}_{0.01}\text{PO}_4/\text{C}$ and $\text{LiMn}_{0.8}\text{Fe}_{0.19}\text{Mg}_{0.01}\text{PO}_4/\text{C}$. Cells were charged at 0.1 C to 4.5 V, held at 4.5 V until the current decreased to 0.01 C, and then discharged at various rates (0.1–10 C) to 2.0 V.

works [7,8,10,11,17,19,20], improvement in electrochemical performance of LiMnPO_4 based materials often made use of nanoparticles and/or a large amount of carbon coating which are clearly undesirable for commercial application in lithium ion batteries considering the instability, high-voltage and low gravimetric density of LiMnPO_4 . In addition, the excellent rate capability of the present $\text{LiMn}_{0.8}\text{Fe}_{0.19}\text{Mg}_{0.01}\text{PO}_4/\text{C}$ sample provides room for further increasing particle size and/or reducing carbon coating amount to meet the requirement of commercial application. Related works are in progress. Anyway, the above results imply that $\text{LiMn}_{0.8}\text{Fe}_{0.19}\text{Mg}_{0.01}\text{PO}_4/\text{C}$ is possibly utilized into practical application for lithium ion batteries.

4. Conclusions

A new LiMnPO_4 based material, $\text{LiMn}_{0.8}\text{Fe}_{0.19}\text{Mg}_{0.01}\text{PO}_4/\text{C}$, was proposed as a high performance cathode material for lithium ion batteries. Although the obtained sample had larger particle size and lower carbon coating amount as compared to those reported in previous works, it still possessed a high capacity and an impressive rate capability. Our results strongly suggest that the $\text{LiMn}_{0.8}\text{Fe}_{0.19}\text{Mg}_{0.01}\text{PO}_4/\text{C}$ has great potential for commercial application in lithium ion batteries.

Acknowledgements

This work was supported by the Natural Science Foundation of Yunnan Province (No. 2009ZC001X), analysis and testing

foundation of KMUST (No. 2010199), and Key Lab of Advanced Materials in Rare&Precious and Non-ferrous Metals, Ministry of Education, KMUST.

Appendix A. Supplementary data

Supplementary data associated with this article can be found, in the online version, at [doi:10.1016/j.jpowsour.2011.12.046](https://doi.org/10.1016/j.jpowsour.2011.12.046).

References

- [1] A.K. Padhi, K.S. Nanjundaswamy, J.B. Goodenough, *J. Electrochem. Soc.* 144 (1997) 1188–1194.
- [2] A. Yamada, M. Hosoya, S.C. Chung, Y. Kudo, K. Hinokuma, K.Y. Liu, Y. Nishi, *J. Power Sources* 119–121 (2003) 232–238.
- [3] M. Yonemura, A. Yamada, Y. Takei, N. Sonoyama, R. Kanno, *J. Electrochem. Soc.* 151 (2004) A1352–A1356.
- [4] C. Delacourt, L. Laffont, R. Bouchet, C. Wurm, J.B. Leriche, M. Morcrette, J.M. Tarascon, *C. Masquelier, J. Electrochem. Soc.* 152 (2005) A913–A921.
- [5] G.H. Li, H. Azuma, M. Tohma, *Electrochem. Solid-State Lett.* 5 (2002) A135–A137.
- [6] C. Delacourt, P. Poizot, M. Morcrette, J.M. Tarascon, C. Masquelier, *Chem. Mater.* 16 (2004) 93–99.
- [7] Z. Bakenov, I. Taniguchi, *J. Power Sources* 195 (2010) 7445–7451.
- [8] S.M. Oh, S.W. Oh, C.S. Yoon, B. Scrosati, K. Amine, Y.K. Sun, *Adv. Funct. Mater.* 20 (2010) 3260–3265.
- [9] T. Drezen, N. Kwon, P. Bowen, I. Teerlinck, M. Isono, I. Exnar, *J. Power Sources* 174 (2007) 949–953.
- [10] D.Y. Wang, H. Buqa, M. Cruzet, G. Deghenghi, T. Drezen, I. Exnar, N.H. Kwon, J.H. Miners, L. Poletto, M. Grätzel, *J. Power Sources* 189 (2009) 624–628.
- [11] D. Choi, D.H. Wang, I.T. Bae, J. Xiao, Z.M. Nie, W. Wang, V.V. Viswanathan, Y.J. Lee, J.G. Zhang, G.L. Graff, Z.G. Yang, J. Liu, *Nano Lett.* 10 (2010) 2799–2805.
- [12] G.Y. Chen, J.D. Wilcox, T.J. Richardson, *Electrochem. Solid-State Lett.* 11 (2008) A190–A194.

- [13] T. Shiratsuchi, S. Okada, T. Doi, J.I. Yamaki, *Electrochim. Acta* 54 (2009) 3145–3151.
- [14] D.Y. Wang, C.Y. Ouyang, T. Drezen, I. Exnar, A. Kay, N.H. Kwon, P. Guerec, J.H. Miners, M.K. Wang, M. Gratzel, *J. Electrochem. Soc.* 157 (2010) A225–A229.
- [15] Z. Bakenov, I. Taniguchi, *J. Electrochem. Soc.* 157 (2010) A430–A436.
- [16] J.W. Lee, M.S. Park, B. Anass, J.H. Park, M.S. Paik, S.G. Doo, *Electrochim. Acta* 55 (2010) 4162–4169.
- [17] J. Kim, D.H. Seo, S.W. Kim, Y.U. Park, K. Kang, *Chem. Commun.* 46 (2010) 1305–1307.
- [18] G. Yang, H. Ni, H. Liu, P. Gao, H. Ji, S. Roy, J. Pinto, X. Jiang, *J. Power Sources* 196 (2011) 4747–4755.
- [19] S.K. Martha, J. Grinblat, O. Haik, E. Zinigrad, T. Drezen, J.H. Miners, I. Exnar, A. Kay, B. Markovsky, D. Aurbach, *Angew. Chem. Int. Ed.* 48 (2009) 8559–8563.
- [20] H. Wang, Y. Yang, Y. Liang, L. Cui, H. Sanchez Casalongue, Y. Li, G. Hong, Y. Cui, H. Dai, *Angew. Chem. Int. Ed.* 50 (2011) 7364–7368.
- [21] S.W. Kim, J. Kim, H. Gwon, K. Kang, *J. Electrochem. Soc.* 156 (2009) A635–A638.
- [22] G. Chen, T.J. Richardson, *J. Power Sources* 195 (2010) 1221–1224.
- [23] S. Ping Ong, A. Jain, G. Hautier, B. Kang, G. Ceder, *Electrochem. Commun.* 12 (2010) 427–430.
- [24] S.K. Martha, O. Haik, E. Zinigrad, I. Exnar, T. Drezen, J.H. Miners, D. Aurbach, *J. Electrochem. Soc.* 158 (2011) A1115–A1122.
- [25] D. Choi, J. Xiao, Y.J. Choi, J.S. Hardy, M. Vijayakumar, J. Liu, W. Xu, W. Wang, J.G. Zhang, G.L. Graff, Z. Yang, *Energy Environ. Sci.* 4 (2011) 4560–4566.
- [26] J. Xiao, N.A. Chernova, S. Upreti, X. Chen, Z. Li, Z. Deng, D. Choi, W. Xu, Z. Nie, G.L. Graff, J. Liu, M.S. Whittingham, J.G. Zhang, *Phys. Chem. Chem. Phys.* 13 (2011) 18099–18106.
- [27] C.L. Hu, H.H. Yi, H.S. Fang, B. Yang, Y.C. Yao, W.H. Ma, Y.N. Dai, *Electrochem. Commun.* 12 (2010) 1784–1787.
- [28] H.H. Yi, C.L. Hu, H.S. Fang, B. Yang, Y.C. Yao, W.H. Ma, Y.N. Dai, *Electrochim. Acta* 56 (2011) 4052–4057.
- [29] J. Hong, F. Wang, X.L. Wang, J. Graetz, *J. Power Sources* 196 (2011) 3659–3663.